Quantum Signature of Analog Hawking Radiation in Momentum Space

D. Boiron,[1] A. Fabbri,[2,3,4,5,*] P.-É. Larré,[6] N. Pavloff,[7,†] C. I. Westbrook,[1] and P. Ziń[8]
[1]Laboratoire Charles Fabry, Institut d'Optique-CNRS-Univ. Paris-Sud, 2 Avenue Augustin Fresnel, 91127 Palaiseau, France
[2]Centro Studi e Ricerche E. Fermi, Piazza del Viminale 1, 00184 Roma, Italy
[3]Dipartimento di Fisica dell'Università di Bologna, Via Irnerio 46, 40126 Bologna, Italy
[4]Departamento de Fisica Teorica and IFIC, Universidad de Valencia-CSIC, C. Dr. Moliner 50, 46100 Burjassot, Spain
[5]Laboratoire de Physique Théorique, CNRS UMR 8627, Bât. 210, Univ. Paris-Sud, 91405 Orsay Cedex, France
[6]INO-CNR BEC Center and Dipartimento di Fisica, Università di Trento, Via Sommarive 14, 38123 Povo, Italy
[7]Laboratoire de Physique Théorique et Modèles Statistiques, CNRS, Univ. Paris Sud, UMR 8626, 91405 Orsay Cedex, France
[8]National Centre for Nuclear Research, ul. Hoża 69, 00-681 Warsaw, Poland
(Received 2 March 2015; published 6 July 2015)

We consider a sonic analog of a black hole realized in the one-dimensional flow of a Bose-Einstein condensate. Our theoretical analysis demonstrates that one- and two-body momentum distributions accessible by present-day experimental techniques provide clear direct evidence (i) of the occurrence of a sonic horizon, (ii) of the associated acoustic Hawking radiation, and (iii) of the quantum nature of the Hawking process. The signature of the quantum behavior persists even at temperatures larger than the chemical potential.

DOI: 10.1103/PhysRevLett.115.025301 PACS numbers: 67.85.De, 04.70.Dy

Forty years ago Hawking [1] discovered that black holes are not completely "black", as general relativity predicts, but emit particles in the form of thermal radiation at the characteristic temperature $T_H = \kappa/2\pi c_\ell$, where c_ℓ is the speed of light and κ the horizon's surface gravity (we use units such that $\hbar = k_B = 1$). This subtle quantum mechanical effect can be understood as arising from a pair-production process in the near-horizon region, in which one member of the pair gets trapped inside the black hole, leaving the other "free" to propagate outside and reach infinity. Unfortunately, it seems impossible to observe Hawking radiation in the astrophysical context, because in ordinary situations of gravitational collapse T_H is much lower than the temperature of the microwave background radiation [2]. Different scenarios have been proposed that would allow the formation of low-mass black holes with higher values of T_H, but they remain speculative. Among these are the suggestions that mini black holes might have been seeded by density fluctuations in the early Universe [3], or could be formed at particle accelerators due to the existence of large extra dimensions [4].

In 1981 Unruh [5] used the mathematical equivalence between the propagation of light in a gravitational black hole and that of sound in a fluid undergoing a subsonic-supersonic transition (henceforth denoted as an "acoustic black hole") to predict, using Hawking's original analysis, that acoustic black holes will emit a thermal flux of phonons (analog Hawking radiation) from their acoustic horizon. Several physical systems have since been proposed to detect the analog of Hawking radiation. Recent investigations attempted to realize acoustic horizon in water tanks experiments [6], via ultrashort pulses in optical fibers [7] or in a transparent Kerr medium [8], by propagating coherent light in nonlinear media [9], in the flow of microcavity polaritons [10], and in atomic Bose-Einstein condensates (BECs) [11], see Fig. 1.

Because of their low temperatures, BECs offer particularly favorable experimental conditions [12], since one can reach situations in which T_H is only one order of magnitude lower than the background temperature in typical ultracold atomic-vapor experiments. This is a significant improvement with respect to the gravitational case, but it still seems too low to attempt a direct detection of the emitted phonons. Fortunately, acoustic black holes have another advantage compared to gravitational ones: the interior of the analog black hole (region of supersonic flow) is accessible to experiments. One can then test the existence of the Hawking effect through the basic pair-production process of Hawking quanta (in the exterior of the acoustic black hole) and of their partners (in the interior). It was

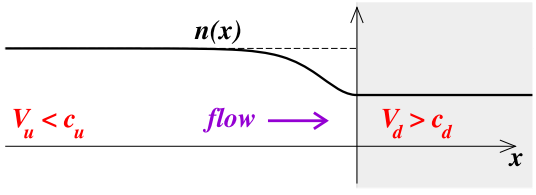

FIG. 1 (color online). Schematic representation of an acoustic black hole in a BEC. The density profile $n(x)$ is the black solid line. V_u and c_u (V_d and c_d) are the asymptotic upstream (downstream) flow and sound velocities. The upstream (downstream) asymptotic flow is subsonic (supersonic). The interior of the analog black hole is shaded in this figure and in Fig. 2.

shown in [13] that this process features characteristic peaks in the correlation function of the density fluctuations and that these peaks exist in BECs. A signature of the Hawking effect, amplified by a laser-type instability [14] in a black-hole–white-hole setting, has been recently observed in Ref. [15].

In the present Letter we consider new observables, namely the one- and two-body momentum distributions, and show that they yield a direct signature of the Hawking effect and of its quantum nature. The motivation for our approach comes from the recent experiment [16] where momentum correlators were used to observe the acoustic analogue of the dynamical Casimir effect [17], a pair-creation process bearing strong analogies with the Hawking effect, in which correlated particles are created in a homogeneous system by a rapid temporal modulation of the system's Hamiltonian. The momentum correlations are particularly interesting because, as shown below, they offer a signature of the quantum nature of the Hawking effect much less affected by the background temperature T than the real-space correlation signal—of intrinsically hydrodynamic nature [13]—which has been recently studied in the $T = 0$ limit [18].

What we denote as an analog black hole is a stationary one-dimensional (1D) flow in which the asymptotic upstream velocity is subsonic and the asymptotic downstream velocity is supersonic. Such configurations, from idealized to more realistic ones, have been proposed in Refs. [13,19–23]. It has been experimentally demonstrated in Ref. [11] and theoretically shown in Ref. [24] how some could be reached by a dynamical process. One of these configurations is schematically represented in Fig. 1. The sonic horizon is the place where the velocity of the flow equals the speed of sound.

In such a structure, the dynamics of elementary excitations is encoded in a S matrix that describes how modes incoming from infinity (upstream or downstream) are scattered by the horizon [20,21]. Far from the horizon, the flow is uniform (with constant velocity and density) and the distant incoming and outgoing modes are thus plane waves. Their lab-frame dispersion relations are of the Bogoliubov type (for the excitations propagating on top of a uniform condensate, see, e.g., [25]), Doppler shifted by the background flow velocity,

$$(\omega - V_{(u/d)}k)^2 = c^2_{(u/d)}k^2\left(1 + \frac{1}{4}k^2\xi^2_{(u/d)}\right). \qquad (1)$$

In this expression ω is the frequency of the plane wave, k its momentum relative to the background flow, and $\xi_{(u/d)} = 1/mc_{(u/d)}$ is the (upstream or downstream) healing length. The dispersion relations (1) are represented in Fig. 2, where upstream and downstream modes are denoted as "u" and "d". We follow the conventions of Refs. [21,23] and label the modes as "in" (such as, for instance, $d1_{\rm in}$) or "out" (such as $u_{\rm out}$) depending on whether their group velocity points toward the horizon (for the "in" modes) or away from the horizon (for the "out" modes), as pictorially described in the lower part of Fig. 2. In the upstream subsonic region the dispersion relation is qualitatively similar to that of a condensate at rest, with one ingoing and one outgoing u channel; new modes appear in the downstream supersonic region where we have two ingoing and two outgoing modes, denoted as $d1$ and $d2$. The new $d2$ modes have negative norm (see, e.g., [26]). From this analysis one can identify the three relevant scattering channels (each is initiated by one of the three ingoing modes) and compute the coefficients of the S matrix [21,23]. This, in turn, makes it possible to expand the creation and annihilation operators $\hat{\psi}^\dagger(p)$ and $\hat{\psi}(p)$ on the scattering channel operators and to determine the population operator $\hat{n}(p) = \hat{\psi}^\dagger(p)\hat{\psi}(p)$ of the state with lab-frame momentum $p = k + mV_{(u/d)}$, where k is the relative momentum of Eq. (1).

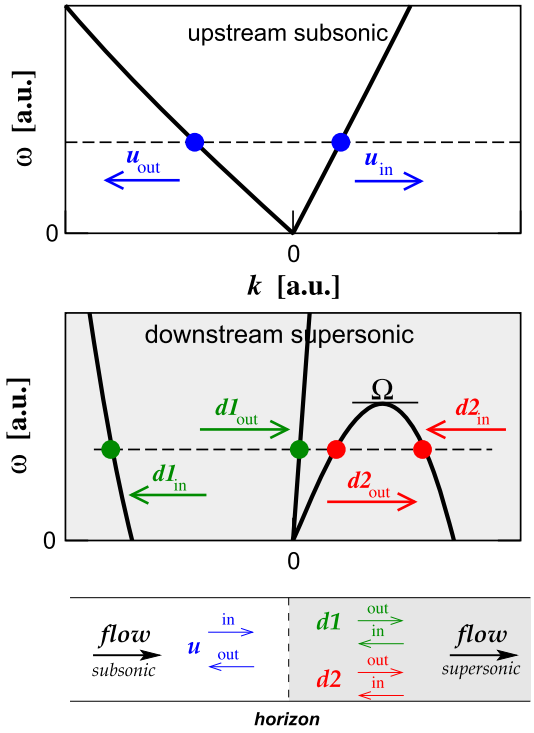

FIG. 2 (color online). Two upper plots: upstream and downstream dispersion relations $\omega(k)$ [from Eq. (1)]. In each plot the horizontal dashed line is fixed by the chosen value of ω. The labeling of the modes is explained in the text; their direction of propagation is represented by an arrow. u and $d1$ modes ($d2$ modes) have a positive (negative) norm. The $d2$ modes disappear for $\omega > \Omega$. The lower plot schematically represents the black-hole configuration in real space and the different modes bearing propagation of elementary excitations.

It is important to present the experimental detection scheme used for measuring the momentum distribution, because this precisely defines how the quantities described

in the present Letter should be theoretically evaluated. The detection employed in Ref. [16] that motivates our approach consists of opening the trap and letting the elementary excitations be converted into particles expelled from both ends of the condensate, according to a process known as "phonon evaporation" [27]. As demonstrated in Ref. [16], after an adiabatic opening of the trapping potential, a measure of the velocity distribution of these particles gives access to the momentum distribution $\langle \hat{n}(p) \rangle$ within the condensate and to the correlator g_2 defined below in Eq. (2) [28].

Figure 3 displays the one-body momentum distribution $\langle \hat{n}(p) \rangle$ corresponding to the above-defined procedure in the $T = 0$ limit. The top part of this figure sketches the expected typical experimental result. The shaded peaks are the upstream and downstream momentum distribution of the condensate, centered around P_u and P_d ($P_{(u/d)} = mV_{(u/d)}$). The lower part of the figure displays our theoretical results obtained within the so-called "waterfall configuration" where the sonic horizon is induced by an external potential step [23]. Very similar results are obtained for another realistic configuration (denoted as "δ-peak configuration" in Ref. [23]) where the horizon is induced by a sharply localized potential. In our theoretical description, the system behaves as a perfect 1D BEC (see the discussion at the end of the Letter). In this case the components of the momentum distribution corresponding to the condensate (the dashed lines at $p = P_u$ and $p = P_d$ in the lower part of Fig. 3) are sharp δ distributions; they are not broadened by phase fluctuations and finite experimental resolution as in the top panel.

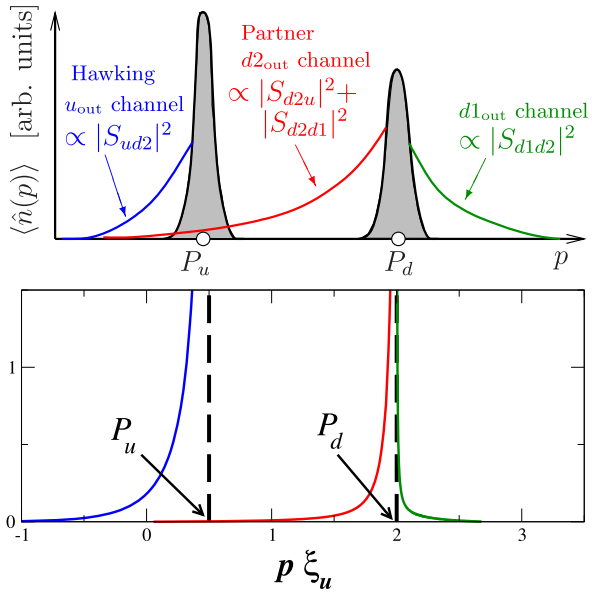

FIG. 3 (color online). Momentum distribution $\langle \hat{n}(p) \rangle$ within the condensate. The figure is drawn in the $T = 0$ limit. The top panel is a schematic representation of a typical experimental result. The lower panel displays the analytic result in the waterfall configuration with $V_u/c_u = 0.5$, $V_d/c_d = 4 = V_d/V_u$. The thick vertical dashed lines correspond to the upstream and downstream condensates located at $p = P_u$ and $p = P_d$ (where here $P_u\xi_u = 0.5$ and $P_d\xi_u = 2$).

It is noteworthy that the presence or absence of a horizon can be inferred from the structure of the one-body momentum distribution $\langle \hat{n}(p) \rangle$. As illustrated in Fig. 3, when a horizon is present, one has two peaks with $P_d > P_u$. On the other hand, without a horizon, one always has $P_d \leq P_u$, the equality being realized in the δ-peak configuration [31].

The side distributions around the peaks in Fig. 3 are signatures of the quantum fluctuations and are proportional to the elements of the S matrix (S_{ud2} is, for instance, the complex and ω-dependent scattering amplitude describing the scattering from the ingoing downstream channel $d2_{\rm in}$ towards the outgoing upstream channel $u_{\rm out}$). In particular, the left shoulder of the peak around P_u in Fig. 3 corresponds to the Hawking quanta escaping from the horizon along the $u_{\rm out}$ channel, and the left shoulder of the peak around P_d to their partners ($d2_{\rm out}$ channel) [32]. At $T = 0$, the existence of these shoulders stems directly from the Hawking effect; they disappear in the absence of the horizon.

We now consider the normally ordered momentum correlation function (two-body signal)

$$g_2(p,q) = \frac{\langle :\hat{n}(p)\hat{n}(q): \rangle}{\langle \hat{n}(p) \rangle \langle \hat{n}(q) \rangle}. \tag{2}$$

Instead of presenting here the detailed analytical evaluation of g_2 corresponding to the different possible steps of the experimental procedure that our theoretical approach is able to describe (see Ref. [31]), we, rather, graphically display g_2 at $T = 0$ in Fig. 4. This plot exhibits the genuine Hawking correlations: in the absence of a horizon, the $T = 0$ normal-ordered g_2 would be uniformly equal to 1. In our stationary setting, spontaneous particle creation *à la* Hawking is triggered by the existence of the negative-norm $d2_{\rm in}$ mode. The process is possible within an energy-conserving framework because the $d2$ modes carry a negative energy [33,34]. Hence, the observation of the new correlation lines $u_{\rm out} - d2_{\rm out}$, $d1_{\rm out} - d2_{\rm out}$, and $u_{\rm out} - d1_{\rm out}$ is direct evidence of the existence of the negative-norm (negative-energy) $d2$ modes and of a region of supersonic flow. As discussed below, we work within a perfect condensate approximation where the momenta are exactly δ correlated along these curves. Compared to the one-body signal displayed in Fig. 3, the measure of the momentum correlation function has the advantage of yielding a signal located around easily identifiable curves. These curves—and therefore the Hawking process—terminate at momenta for which the $d2$ modes disappear: this corresponds to the regime where $\omega > \Omega$ in Fig. 2.

Let us now turn to the quantitative study of the nature of correlations along the lines identified in Fig. 4. The

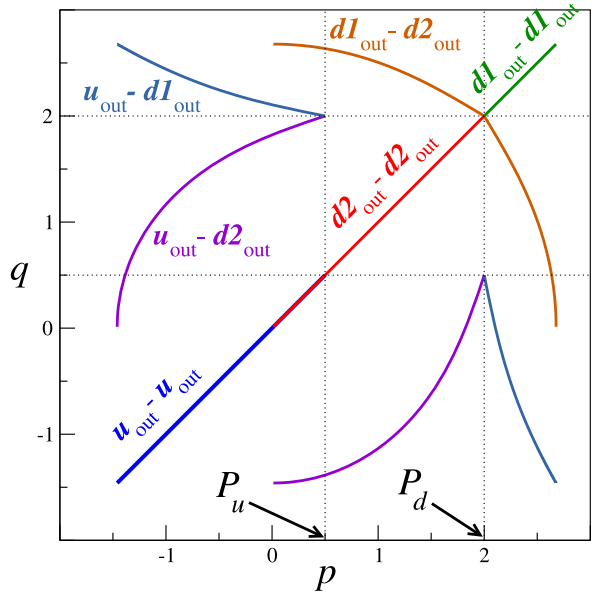

FIG. 4 (color online). Momentum-correlation pattern of $g_2(p,q)$ in the presence of a black-hole horizon at $T=0$. This plot is drawn for the same configuration and the same parameters as the lower panel of Fig. 3. The dotted lines are the momenta of the upstream and downstream condensates (P_u and P_d). The momenta are expressed in units of ξ_u^{-1}. Except for the colored correlation lines, $g_2(p,q)$ is uniformly equal to 1. The colors are used for a nonambiguous identification of the correlation lines. As is obvious from the definition (2), the figure is symmetric with respect to the diagonal.

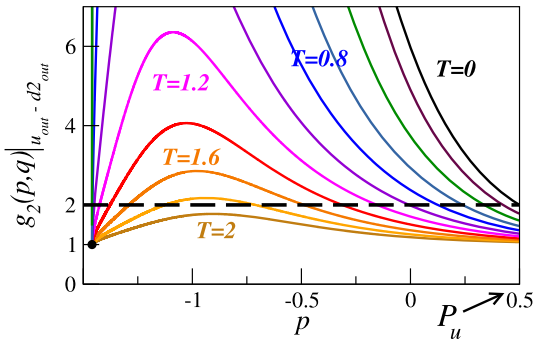

FIG. 5 (color online). The value of $g_2(p,q)$ along the $u_{\rm out}-d2_{\rm out}$ correlation line (violet line in Fig. 4) is plotted as a function of p (expressed in units of ξ_u^{-1}) for different temperatures. The Cauchy-Schwarz inequality is violated when $g_2(p,q)$ is larger than 2. The temperatures are expressed in units of the upstream chemical potential mc_u^2 ($0 \le T \le 2$). For the set of parameters chosen here and in the previous figures, the Hawking temperature is $T_H = 0.134$.

occurrence of entanglement and the quantum nature of the Hawking process can be tested through the violation of the Cauchy-Schwarz inequality, as recently studied in a similar context in Refs. [35]. More specifically, the Cauchy-Schwarz inequality is violated along the characteristic Hawking quanta–partner correlation lines $u_{\rm out}-d2_{\rm out}$ of Fig. 4 if (see, e.g., [36])

$$g_2(p,q)|_{u_{\rm out}-d2_{\rm out}} > \sqrt{g_2(p,p)|_{u_{\rm out}} \times g_2(q,q)|_{d2_{\rm out}}}. \quad (3)$$

In Fig. 5 this corresponds to the region located above the dashed horizontal black line. In the Bogoliubov approach used in the present Letter, Wick's theorem yields $g_2(p,p)|_{u_{\rm out}} = g_2(q,q)|_{d2_{\rm out}} = 2$ for all temperatures; as a result, the right-hand side of inequality (3) is equal to 2. The computations are done in a setting where the system is in an initial thermal state at temperature $T \neq 0$, and where the population of quasiparticles is adiabatically converted into real particles upon opening the trap. As expected, the region of violation of the Cauchy-Schwarz inequality decreases when T increases [37], but even at relatively high temperatures ($T > 1.5mc_u^2$ and $> 10T_H$) the momentum correlation signal remains a clear signature for revealing the quantum nature of the Hawking signal [38].

Finally, it is important to stress that the results presented in this Letter are obtained within a Bogoliubov approximation assuming perfect condensation of the 1D Bose system. This approximation is valid in an intermediate density regime—denoted as "1D mean field" in Ref. [39]—where the system is accurately described by an order parameter obeying an effective 1D Gross-Pitaevskii equation. At low density, phase fluctuations destroy the long-range order and the possibility of a true Bose-Einstein condensate, and blur the sharp correlations of Fig. 4 [40]. At large density, phase fluctuations can be neglected, but one cannot omit the effect of transverse confinement, which induces a modification of the dispersion relation and creates new transverse dispersion modes [41], resulting in the appearance of new correlation lines in Fig. 4. One should, however, keep in mind that for a typical system (say, ^{87}Rb, ^{23}Na, or ^{4}He atoms in a guide with a transverse confinement of angular frequency $\omega_\perp = 2\pi \times 500$ Hz) the 1D mean-field approximation used in the present Letter is quite relevant because it holds for a range of linear densities varying over 4 orders of magnitude [42].

This work was supported by the French ANR under Grant No. ANR-11-IDEX-0003-02 (Inter-Labex Grant QEAGE), by the Triangle de la Physique, and by the Institut Francilien pour la Recherche en Atomes Froids. P. Z. was supported by the National Science Centre Grant No. DEC-2011/03/D/ST2/00200.

*Corresponding author.
afabbri@ific.uv.es
†Corresponding author.
nicolas.pavloff@u-psud.fr

[1] S. W. Hawking, Nature (London) **248**, 30 (1974); Commun. Math. Phys. **43**, 199 (1975).

[2] From the surface gravity formula, one obtains $T_H \simeq 10^{-7} M^{-1}$ K, where M is the mass of the black hole expressed in units of the mass of the Sun.

[3] B. J. Carr, Astrophys. J. **201**, 1 (1975).

[4] N. Arkani-Hamed, S. Dimopoulos, and G. R. Dvali, Phys. Lett. B **429**, 263 (1998); L. Randall and R. Sundrum, Phys. Rev. Lett. **83**, 3370 (1999).

[5] W. G. Unruh, Phys. Rev. Lett. **46**, 1351 (1981).

[6] S. Weinfurtner, E. W. Tedford, M. C. J. Penrice, W. G. Unruh, and G. A. Lawrence, Phys. Rev. Lett. **106**, 021302 (2011).

[7] T. G. Philbin, C. Kuklewicz, S. Robertson, S. Hill, F. Konig, and U. Leonhardt, Science **319**, 1367 (2008).

[8] F. Belgiorno, S. L. Cacciatori, M. Clerici, V. Gorini, G. Ortenzi, L. Rizzi, E. Rubino, V. G. Sala, and D. Faccio, Phys. Rev. Lett. **105**, 203901 (2010).

[9] M. Elazar, V. Fleurov, and S. Bar-Ad, Phys. Rev. A **86**, 063821 (2012).

[10] H. S. Nguyen, D. Gerace, I. Carusotto, D. Sanvitto, E. Galopin, A. Lemaître, I. Sagnes, J. Bloch, and A. Amo, Phys. Rev. Lett. **114**, 036402 (2015).

[11] O. Lahav, A. Itah, A. Blumkin, C. Gordon, S. Rinott, A. Zayats, and J. Steinhauer, Phys. Rev. Lett. **105**, 240401 (2010).

[12] L. J. Garay, J. R. Anglin, J. I. Cirac, and P. Zoller, Phys. Rev. Lett. **85**, 4643 (2000); Phys. Rev. A **63**, 023611 (2001).

[13] R. Balbinot, A. Fabbri, S. Fagnocchi, A. Recati, and I. Carusotto, Phys. Rev. A **78**, 021603 (2008); I. Carusotto, S. Fagnocchi, A. Recati, R. Balbinot, and A. Fabbri, New J. Phys. **10**, 103001 (2008).

[14] S. Corley and T. Jacobson, Phys. Rev. D **59**, 124011 (1999); A. Coutant and R. Parentani, Phys. Rev. D **81**, 084042 (2010); S. Finazzi and R. Parentani, New J. Phys. **12**, 095015 (2010).

[15] J. Steinhauer, Nat. Phys. **10**, 864 (2014).

[16] J.-C. Jaskula, G. B. Partridge, M. Bonneau, R. Lopes, J. Ruaudel, D. Boiron, and C. I. Westbrook, Phys. Rev. Lett. **109**, 220401 (2012).

[17] S. A. Fulling and P. C. W. Davies, Proc. R. Soc. A **348**, 393 (1976); I. Carusotto, R. Balbinot, A. Fabbri, and A. Recati, Eur. Phys. J. D **56**, 391 (2010).

[18] J. Steinhauer, arXiv:1504.06583.

[19] U. Leonhardt, T. Kiss, and P. Ohberg, J. Opt. B **5**, S42 (2003).

[20] J. Macher and R. Parentani, Phys. Rev. A **80**, 043601 (2009).

[21] A. Recati, N. Pavloff, and I. Carusotto, Phys. Rev. A **80**, 043603 (2009).

[22] I. Zapata, M. Albert, R. Parentani, and F. Sols, New J. Phys. **13**, 063048 (2011).

[23] P.-É. Larré, A. Recati, I. Carusotto, and N. Pavloff, Phys. Rev. A **85**, 013621 (2012).

[24] A. M. Kamchatnov and N. Pavloff, Phys. Rev. A **85**, 033603 (2012).

[25] L. Pitaevskii and S. Stringari, *Bose-Einstein Condensation* (Clarendon Press, Oxford, 2003).

[26] A. L. Fetter, in *Bose-Einstein Condensation in Atomic Gases, Proceedings of the International School of Physics "Enrico Fermi," course CXL*, edited by M. Inguscio, S. Stringari, and C. E. Wieman (IOS Press, Amster-dam, 1999), p. 201.

[27] C. Tozzo and F. Dalfovo, Phys. Rev. A **69**, 053606 (2004).

[28] One can also imagine performing measurements of the momentum of the excitations by using two consecutive Bragg pulses as proposed in Ref. [29] and performed in Ref. [30]. However, it seems challenging to precisely measure correlations with this procedure.

[29] A. Brunello, F. Dalfovo, L. P. Pitaevskii, and S. Stringari, Phys. Rev. Lett. **85**, 4422 (2000).

[30] J. M. Vogels, K. Xu, C. Raman, J. R. Abo-Shaeer, and W. Ketterle, Phys. Rev. Lett. **88**, 060402 (2002).

[31] D. Boiron, A. Fabbri, P.-É. Larré, N. Pavloff, C. I. Westbrook, and P. Ziń (to be published).

[32] After removing the external potentials, the acoustic horizon disappears, the collective excitations correspondingly transform into real particles, and the Hawking partners (within the $d2_{\mathrm{out}}$ channel) propagate with a lab-frame momentum $p = P_d - k$ smaller than P_d, thus contributing to $\langle \hat{n}(p) \rangle$ with a shoulder at the left of P_d in Fig. 3.

[33] R. Balbinot, I. Carusotto, A. Fabbri, C. Mayoral, and A. Recati, Lect. Notes Phys. **870**, 181 (2013).

[34] S. J. Robertson, J. Phys. B **45**, 163001 (2012).

[35] K. V. Kheruntsyan, J.-C. Jaskula, P. Deuar, M. Bonneau, G. B. Partridge, J. Ruaudel, R. Lopes, D. Boiron, and C. I. Westbrook, Phys. Rev. Lett. **108**, 260401 (2012); D. E. Bruschi, N. Friis, I. Fuentes, and S. Weinfurtner, New J. Phys. **15**, 113016 (2013); J. R. M. de Nova, F. Sols, and I. Zapata, Phys. Rev. A **89**, 043808 (2014); X. Busch, I. Carusotto, and R. Parentani, Phys. Rev. A **89**, 043819 (2014); X. Busch and R. Parentani, Phys. Rev. D **89**, 105024 (2014); S. Finazzi and I. Carusotto, Phys. Rev. A **90**, 033607 (2014); T. Wasak, P. Szańkowski, P. Ziń, M. Trippenbach, and J. Chwedeńczuk, Phys. Rev. A **90**, 033616 (2014).

[36] D. F. Walls and G. J. Milburn, *Quantum Optics* (Springer-Verlag, New York, 2008).

[37] In particular, even for small temperatures, the Cauchy-Schwarz inequality is not violated in the hydrodynamic $p\xi_u \sim 0.5$ regime or in the region $p\xi_u \simeq -1.46$, where Hawking radiation shuts off and is easily superseded by thermal effects.

[38] Entanglement is also present along the $d1_{\mathrm{out}} - d2_{\mathrm{out}}$ correlation lines, but is less easily detected, and is absent along the $u_{\mathrm{out}} - d1_{\mathrm{out}}$ lines.

[39] C. Menotti and S. Stringari, Phys. Rev. A **66**, 043610 (2002).

[40] L. Mathey, A. Vishwanath, and E. Altman, Phys. Rev. A **79**, 013609 (2009); I. Bouchoule, M. Arzamasovs, K. V. Kheruntsyan, and D. M. Gangardt, Phys. Rev. A **86**, 033626 (2012).

[41] E. Zaremba, Phys. Rev. A **57**, 518 (1998); S. Stringari, Phys. Rev. A **58**, 2385 (1998); C. Tozzo and F. Dalfovo, New J. Phys. **5**, 54 (2003).

[42] The 1D mean-field regime holds, at $T = 0$, for linear densities n satisfying $(a/a_\perp)^2 \ll na \ll 1$ where $a_\perp = (\hbar/m\omega_\perp)^{1/2}$ and a is the 3D s-wave scattering length. In the examples chosen in the text the ratio $a/a_\perp$ is roughly of order 10^{-2} and n should thus satisfy $10^{-4} \ll na \ll 1$.